Modeling Interactions between Trypanothione and Antimony-Oxide Clusters

Hassan Rabaa[a], Andriy Grafov[b] and Dage Sundholm[b,*]

[a] *Department of Chemistry, Ibn Tofail University, ESCTM, P.O. Box 133, 14000, Kenitra, Morocco. Email: hrabaa@yahoo.com (MA)*

[b] *Department of Chemistry, Faculty of Science, University of Helsinki, P.O. B. 55, FIN-00014, Finland. Email: dage.sundholm@helsinki.fi (FIN)*

** Corresponding author, sundholm@chem.helsinki.fi*

† Dedicated to Emeritus Jean-Yves Saillard professor at Rennes 1 University (France)

Interactions of antimony-oxide clusters with trypanothione have been modelled to understand their inhibitory activity against leishmaniasis. Trypanothione is essential for the survival of leishmania parasites because it is responsible for maintaining their cellular thiol-disulfide redox regulation. Density functional theory (DFT) calculations show that the Sb^{V} oxide clusters form hydrogen bonds from the oxygens to the amine and carboxyl group of the trypanothione. The reaction between trypanothione and the Sb^{V} oxide cluster does not break the S-S bond of trypanothione, whereas the reaction with antimony-oxide clusters containing at least one Sb^{III} atom leads to dissociation of the S-S bond of both the oxidized and the reduced form of trypanothione suggesting that antimony-oxide clusters with at least one Sb^{III} atom may destroy trypanothione that is vital for the parasite metabolism.

Introduction

Leishmaniasis is a neglected tropical disease caused by protozoan parasites of genus *Leishmania*. The disease occurs mainly in regions with poverty, population displacement, poor housing, and lack of resources. According to the World Health Organization, 98 countries and territories are endemic for leishmaniases[1]. Annually, the number of new leishmaniasis cases is 700 000 – 1 200 000 of which 14 000-40 000 are fatal, making the disease the second major mortality cause among all tropical diseases[2–8].

Despite the development of new ways to treat the decease, antimony-based drugs that was proposed by Vianna[9] more than a century ago are still the most important remedy for all types of leishmaniasis[10–18]. Leishmaniasis is characterised by a unique thiol-based metabolism involving the trypanothione reductase system protecting the parasites from oxidative stress and damage in the mammalian host cells. The action mechanism of antimony-based drugs is either due to interactions of Sb^{V} with ribonucleosides or due to reduction of Sb^{V} prodrugs into Sb^{III} compounds[15–19], which then react with sulfur-containing biomolecules such as trypanothione in the cytosol or with cysteine in the lysosomes[6,7].

Trypanothione is a dipeptide linked via a disulfide bridge. It is synthesized from glutathione and spermidine by trypanothione synthetase and is further reduced by trypanothione reductase (TR) [8,12,14–17,20]. Trypanothione acts as a reducing agent, and it is responsible for maintaining the parasite's cellular thiol-disulfide redox balance.

Fairlamb *et al*. have shown that pentavalent antimony, which is the main drug used against Leishmaniasis in vivo, interferes with the trypanothione metabolism by inducing a rapid efflux of intracellular reduced trypanothione ($T(SH)_2$) and by inhibiting the TR in intact cells[8]. They also found that Sb^{III} induces a rapid efflux of intracellular trypanothione and glutathione as well as inhibits the TR, which is known as one of the key enzymes in *Leishmania* infection[8,12,17]. Although this enzyme is thought to be a potential drug target, development of accurate TR inhibitors is still needed[8,12]. Several metal complexes have been tested on a variety of trypanosomiasis and were shown to be active on different molecular targets[14,17,20]. However, despite those findings the exact mechanisms for the interaction of antimony-based drugs with trypanothione and the inhibition of trypanothione reductase are not well understood[3–5].

Another important aspect of antimonial therapy of leishmaniasis is connected to the severe side effect of the drugs as well as the development of the parasite's resistance to Sb drugs[13,14]. To mitigate the problem by enhancing the drug efficiency and to reduce its toxicity[21,22], one of us proposed treatments using $Sb_2O_5{\cdot}nH_2O$ nanoparticles (SbNP), whose surface was modified with N-methylglucamine[23,24].

Antimony is often considered as a semimetal, with the most common oxidation states being trivalent Sb^{III} and pentavalent Sb^{V}. Different mechanistic theoretical studies have been reported, where small organic molecules and antimony were used for assessing the inhibition activity[25–29].

In this work, we computationally model hydrated antimony-oxide clusters at the density functional theory (DFT) level using the Gaussian 16 [30] and Turbomole 7.3 [31,32] programs. Interactions with the SbNP were

simulated by performing calculations on antimony-oxide cluster models coordinated to trypanothione. The aim is to elucidate how antimony-oxide clusters react with trypanothione and how antimony clusters may participate in the inhibition process against *Leishmania* parasites.

Computational methodology

The molecular structures and thermodynamic properties of the studied molecules were calculated at the density functional theory (DFT) level using the TPSS functional[33], def2-TZVP basis sets[34], and the D3(BJ) semi-empirical dispersion correction[35]. The Stuttgart effective core potential was used for Sb[36]. The molecular structures were optimized in the gas phase as well as using the SMD continuum solvation model[37,38] that considers interactions of hydroxylated antimony oxides clusters with the trypanothione dipeptide in aqueous solution. The initial cluster structure was taken from the X-ray data of Sb_2O_5 [39,40]. The Cartesian coordinates of the molecular structures optimized in the gas phase are given as Supporting Information (SI)

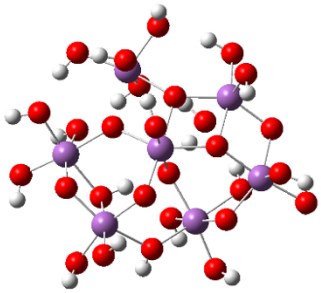

Figure 1: The optimized molecular structure of $[Sb_7O_{28}H_{21}]$ (**A**). The Sb atoms are lilac, the O atoms are red, and the H atoms are light grey.

The cluster neutrality was maintained by adding protons to the terminal oxygens of the cluster model $[Sb_7O_{28}H_{21}]$ (A) shown in Figure 1. The trypanothione/cluster complexes were constructed by adding the molecules to different sides of the cluster. In the initial molecular structure, the trypanothione molecule was coplanar with its main axis parallel to the long axis of the cluster. The complex was optimized at the TPSS/def2-TZVP/D3(BJ) level. The calculated harmonic frequencies were positive verifying that the obtained stationary points are minima on the potential energy surface. A singlet spin state was assumed, and no symmetry constraints were imposed.

Results and discussion

Calculations on $[Sb_7O_{28}H_{21}]$

The inhibitor effect of antimony oxide was studied by performing DFT calculations at the TPSS/def2-TZVP/D3(BJ) level on the $[Sb_7O_{28}H_{21}]$ and trypanothione in vacuum as well as in water medium. The octahedral environment of the antimony centres was preserved in the optimization. The Sb-O bond distances of the cluster were in the range of 1.913-2.085 Å and the O-Sb-O angles are 110°-116°, which agree well with X-ray data[41]. The Mulliken charges of the antimony atoms were 2.13-2.26 *e* and -0.78 to -1.8 *e* for the oxygen atoms. The HOMO/LUMO energies of (**A**) in the gas phase and in water solution were -8.01/-3.91 eV and -8.82/-4.27 eV, respectively. The HOMO and the LUMO energies are stabilized by the surrounding polar medium leading to a HOMO-LUMO gap that is about 0.5 eV larger in water than in the gas phase. The polar medium also increases the dipole moment of (**A**) from 7.02 D in the gas phase to 8.52 D in solution.

Calculations on trypanothione

The HOMO/LUMO energies of trypanothione (**B**) shown in Figure 2 are -6.02/-2.57 eV in the gas phase. The aqueous medium stabilizes the LUMO energy by about 1 eV, whereas the HOMO energy is less affected by the polar medium. The HOMO/LUMO energies of (**B**) are -6.28/-3.61 eV in aqueous solution. The Cartesian coordinates of the optimized molecular structure of trypanothione (**B**) are given in the SI.

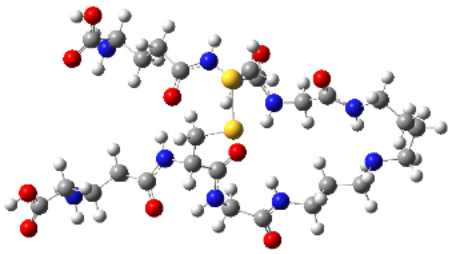

Figure 2. The optimized molecular structure of trypanothione (**B**). The O atoms are red, the N atoms are blue, the S atoms are yellow, the C atoms are grey, and the H atoms are light grey.

Calculations on the $[Sb_7O_{28}H_{21}]$/trypanothione

To understand the inhibition mechanism, we studied the $[Sb_7O_{28}H_{21}]$/trypanothione complex (**C**) shown in the Figure 3. The molecular structure was constructed from the X-ray structure of antimony oxide cluster by adding the trypanothione. The complex was then optimized at the TPSS/def2-TZVP/D3(BJ) level. The Cartesian coordinates of the complex **C** are given in the SI. The main features seen in the cluster structure are the short intermolecular hydrogen bonds between trypanothione and the cluster suggesting that they are bonded strongly[41].Thus, the complex is formed by a partial deprotonation of the amine and hydroxyl groups of trypanothione. The N-H and O-H bonds of trypanothione stretch from the typical bond distances of about 1 Å, they become longer than for the isolated trypanothione molecule by 0.4 Å and 0.7 Å, respectively. The trypanothione is bound to the cluster via several hydrogen-bond bridges where the hydrogen is roughly halfway between the oxygen of the cluster and the nitrogen or the oxygen of trypanothione, suggesting that the hydrogen bonds are strong. The S-S bond of trypanothione is 0.17 Å shorter in the complex. Thus, the main structural change upon complexation is the partial deprotonation of the trypanothione towards the antimony oxide surface without breaking the S-S bond.

Figure 3: The optimized molecular structure of the **$[Sb_7O_{28}H_{21}]$**/trypanothione complex (**C**). The Sb atoms are lilac, the O atoms are red, the N atoms are blue, the S atoms are yellow, the C atoms are grey, and the H atoms are light grey.

The deprotonation was confirmed by changes in the Mulliken charges. The Mulliken charges of N and C are negative, and the charge of Sb is less positive in the complex. The population analysis suggests that 0.3-0.5 electrons are transferred to the Sb atoms when trypanothione binds to the cluster. The frontier orbitals play an important role in the inhibition reaction. The highest occupied molecular orbital (HOMO) and the lowest unoccupied molecular orbital (LUMO) of the complex are localized on the cluster in water medium. In gas phase, the LUMO of the complex is delocalized on the trypanothione moiety and corresponds to the HOMO of trypanothione. The HOMO of the complex is localized to the antimony oxide cluster as shown in Figure 4. Upon complexation, the HOMO of trypanothione is on the lone pairs of the sulfur atoms and the CO and NH_2 moieties donate electron charge to the LUMO of the antimony oxide cluster.

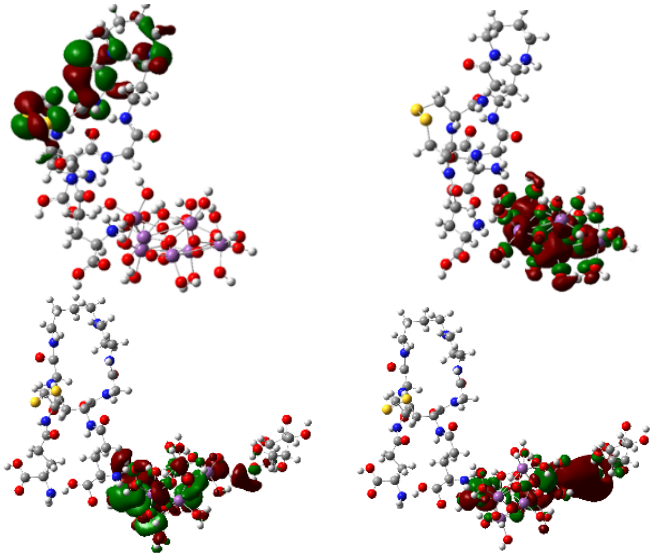

Figure 4: The upper part shows the HOMO (left)-LUMO (right) of the complex (**C**) in gas phase. The lower one is obtained when considering the surrounding water. The Sb atoms are lilac, the O atoms are red, the N atoms are blue, the S atoms are yellow, the C atoms are grey, and the H atoms are light grey.

The HOMO/LUMO energies of the $[Sb_7O_{28}H_{21}]$/ trypanothione complex are -6.4/-1.4 eV in the gas phase yielding a HOMO-LUMO gap of 5 eV, whereas in aqueous solution the HOMO/LUMO energies are -5.7/-4.3 eV yielding a smaller HOMO-LUMO gap of 3.6 eV. The frontier orbitals are located on the cluster in the aqueous solution, whereas in the gas phase, the HOMO is located on trypanothione and the LUMO is on the cluster. The binding free energy (ΔG) of the complex is -70 kcal/mol and -65 kcal/mol in gas phase and water medium, respectively.

The Sb^{V} oxide cluster forms a strongly hydrogen bonded complex with the trypanothione without dissociating the disulfide group. Due to the strong hydrogen bonds between the amine and hydroxyl groups of trypanothione and the oxygens of the cluster it could promote an inhibition process without dissociating the dipeptide. However, it may lead to a complete trypanothione coverage on cluster preventing further reactions.

We also investigated the reaction between the cluster and a reduced form of trypanothione $T(SH)_2$. The molecular structure of the reduced trypanothione optimized at the TPSS/def2-TZVP/D3(BJ) level is shown in Figure 5.

In the experimental studies, there is N-methylglucamine on the surface of the antimony-oxide nanoparticles, which can remove a proton from the cluster surface or from the dipeptide adsorbed on the cluster surface. The deprotonation may change the oxidation state of antimony to Sb^{III} [15–18]. In the calculations, we manually removed a proton from the cluster surface and modelled

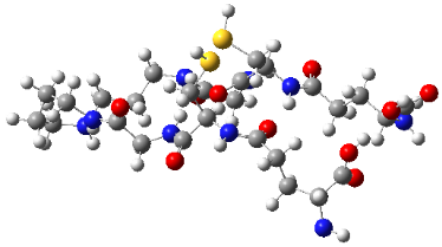

Figure 5: The molecular structure of the reduced form of trypanothione. The S atoms are yellow, O atoms are red, N atoms are blue, C atoms are grey, and the H atoms are light grey.

the reaction with the deprotonated negatively charged cluster. We also considered a modified cluster **A** containing one Sb^{III} atom and its interaction with both the oxidized and the reduced forms of the trypanothione.

The cluster surface was modified by removing oxygen species coordinated to the antimony on the active surface, which also formally changed the oxidation state of one Sb atom from Sb^{V} to Sb^{III}. The Sb^{III} site is then available for reactions with the sulfur atoms of trypanothione. The carbohydrate was not added to the model since we already considered the deprotonation step when constructing the cluster with one Sb^{III} atom. The trypanothione reactions with the cluster containing Sb^{V} atoms only and the one bearing one Sb^{III} atom were completely different. When all Sb atoms on the surface are in the oxidation state Sb^{V}, the trypanothione binds strongly to the cluster surface forming hydrogen bonds between trypanothione and the oxygens of the cluster, whereas the cluster containing Sb^{III} leads to a reaction that breaks the S-S bond of trypanothione independently of whether it is in the oxidized or reduced form. The reaction with the reduced trypanothione breaks the disulfide bridge forming two thiol moieties. The reaction product is bound to the cluster with dipole-dipole interactions. The reaction with trypanothione also breaks the S-S bond and forms a new S-Sb bond between the modified trypanothione and the cluster. The reaction products are shown in the Figure 6.

Experimental observations support the proposed reaction mechanism[15,17]. Breaking the S-S bond of trypanothione affects the intracellular thiol-disulfide redox balance of the parasite, which is essential for its survival in a mammalian host cell[42].

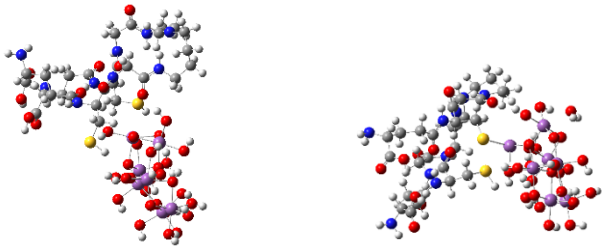

Figure 6: The molecular structures of a complex of reduced trypanothione with $[Sb_7O_{28}H_{21}]$ (left) and a complex of trypanothione with $[Sb_7O_{28}H_{21}]$ (right). The clusters contain one Sb^{III} atom. The Sb atoms are lilac, the O atoms are red, the N atoms are blue, the S atoms are yellow, the C atoms are grey, and the H atoms are light grey.

Conclusions

We carried out DFT calculations at the TPSS-D3/def2-TZVP level on complexes consisting of trypanothione bound to antimony-oxide clusters. The calculations show that there is a strong interaction between trypanothione and the cluster. Trypanothione is linked to the cluster via hydrogen bonds between the amine and hydroxyl groups of the dipeptide and the oxygens of the cluster. Formation of the trypanothione complex with antimony oxide does not lead to any dissociation of the S-S bond when all Sb atoms are in the formal oxidation state of Sb^{V}. Mulliken population analysis shows that trypanothione donates electron charge to the antimony oxide cluster upon complexation. N-methylglucamine on the antimony-oxide cluster can remove a proton from the cluster surface enabling formation of a reactive Sb^{III} centre.

Introducing one Sb^{III} atom in the antimony-oxide cluster changes drastically the reaction pathway with trypanothione. The dissociation of the S-S bond of the dipeptide occurs both for the oxidized and reduced form of trypanothione. The present study suggest that antimony must be in oxidation state Sb^{III} to break the S-S bond of trypanothione, whereas the Sb^{V} oxide cluster strongly binds trypanothione to its surface. Thus, the surface of Sb^{V} oxide clusters will be covered by trypanothione molecules preventing to some extent its redox regulatory ability, whereas antimony clusters containing Sb^{III} break the S-S bond of trypanothione. Since the cluster surface remains clean, the catalytic reaction of the Sb^{III} containing cluster can continue and it can thereby perturb the redox regulation within the parasite cell.

Conflicts of interest

There are no conflicts to declare.

Acknowledgements

The authors gratefully acknowledge the support from the European community through the Horizon 2020 MSCA-RISE-2016-734759 project, acronym VAHVISTUS. HR acknowledges specially the support from the Arab Fund of Kuwait and thanking Drs. R. Hoffmann (Cornell University), T. Cundary (UNT), M. Omary (UNT) for useful discussions. We acknowledge Center of Calculations CASCM (UNT), CSC (the Finnish IT Center for Science) and the Finnish Grid and Cloud Infrastructure (persistent identifier urn:nbn:fi:research-infras-2016072533) for computer time.

References

1 Leishmaniasis, https://www.who.int/news-room/fact-sheets/detail/leishmaniasis.

2 H. L. Choi, S. Jain, J. A. Ruiz Postigo, B. Borisch and D. A. Dagne, *PLoS Negl. Trop. Dis.*, 2021, **15**, e0009181.

3 A. K. Haldar, P. Sen and S. Roy, *Mol. Biol. Int.*, 2011, **2011**, 1–23.

4 L. S. C. Bernardes, C. L. Zani and I. Carvalho, *Curr. Med. Chem.*, 2013, **20**, 2673–2696.

5 L. G. Goodwin, *Trans. R. Soc. Trop. Med. Hyg.*, 1995, **89**, 339–341.

6 P. Desjeux, *Comp. Immunol. Microbiol. Infect. Dis.*, 2004, **27**, 305–318.

7 R. Reithinger, J.-C. Dujardin, H. Louzir, C. Pirmez, B. Alexander and S. Brooker, *Lancet Infect. Dis.*, 2007, **7**, 581–596.

8 A. H. Fairlamb and A. Cerami, *Annu. Rev. Microbiol.*, 1992, **46**, 695–729.

9 G. Vianna, in *7-o Congresso Brasileiro de Medicina Tropical de São Paulo, São Paullo, Brasil*, São Paulo, 1912, pp. 426–428.

10 F. Frézard, C. Demicheli and R. R. Ribeiro, *Molecules*, 2009, **14**, 2317–2336.

11 J. Menezes, T. da Silva, J. dos Santos, E. Catari, M. Meneghetti, C. da Matta, M. Alexandre-Moreira, N. Santos-Magalhães, L. Grillo and C. Dornelas, *Appl. Clay Sci.*, 2014, **91**–**92**, 127–134.

12 S. Wyllie, M. L. Cunningham and A. H. Fairlamb, *J. Biol. Chem.*, 2004, **279**, 39925–39932.

13 Ashutosh, S. Sundar and N. Goyal, *J. Med. Microbiol.*, 2007, **56**, 143–153.

14 M. Mohebali, E. Kazemirad, H. Hajjaran, E. Kazemirad, M. A. Oshaghi, R. Raoofian and A. Teimouri, *Arch. Dermatol. Res.*, 2019, **311**, 9–17.

15 P. Baiocco, G. Colotti, S. Franceschini and A. Ilari, *J. Med. Chem.*, 2009, **52**, 2603–2612.

16 H. Denton, J. C. McGregor and G. H. Coombs, *Biochem. J.*, 2004, **381**, 405–412.

17 M. L. Cunningham and A. H. Fairlamb, *Eur. J. Biochem.*, 1995, **230**, 460–468.

18 W. L. Roberts, J. D. Berman and P. M. Rainey, *Antimicrob. Agents Chemother.*, 1995, **39**, 1234–1239.

19 C. Dos, S. Ferreira, P. Silveira Martins, C. Demicheli, C. Brochu, M. Ouellette and F. Frézard, *BioMetals*, 2003, **16**, 441–446.

20 C. Dumas, M. Ouellette, J. Tovar, M. L. Cunningham, A. H. Fairlamb, S. Tamar, M. Olivier and B. Papadopoulou, *EMBO J.*, 1997, **16**, 2590–2598.

21 D. Cavallo, I. Iavicoli, A. Setini, A. Marinaccio, B. Perniconi, G. Carelli and S. Iavicoli, *Environ. Mol. Mutagen.*, 2002, **40**, 184–189.

22 T. Gebel, *Chem. Biol. Interact.*, 1997, **107**, 131–144.

23 Grafov A., Grafova I., Pereira A.M.R.F., Leskelä M.A. BR 10 2019 005007 1, 2019.

24 A. M. R. Franco, I. Grafova, F. V. Soares, G. Gentile, C. D. C. Wyrepkowski, M. A. Bolson, E. Sargentini Jr, C. Carfagna, M. Leskelä and A. Grafov, *Int. J. Nanomedicine*, 2016, **11**, 6771–6780.

25 N. Süleymanoğlu, Y. Ünver, R. Ustabaş, Ş. Direkel and G. Alpaslan, *J. Mol. Struct.*, 2017, **1144**, 80–86.

26 R. Y. O. Moreira, D. S. B. Brasil, C. N. Alves, G. M. S. P. Guilhon, L. S. Santos, M. S. P. Arruda, A. H. Müller, P. S. Barbosa, A. S. Abreu, E. O. Silva, V.

M. Rumjanek, J. Souza, A. B. F. da Silva and R. H. de A. Santos, *Int. J. Quantum Chem.*, 2008, **108**, 513–520.
27 J. P. do Nascimento, L. S. Santos, R. H. A. Santos, É. Tozzo, J. G. Ferreira, M. C. L. do Carmo, D. S. B. Brasil and C. N. Alves, *J. Braz. Chem. Soc.*, 2010, **21**, 1825–1837.
28 M. M. Mohamed Abdelahi, Y. El Bakri, C.-H. Lai, K. Subramani, E. H. Anouar, S. Ahmad, M. Benchidmi, J. T. Mague, J. Popović-Djordjević and S. Goumri-Said, *J. Enzyme Inhib. Med. Chem.*, 2022, **37**, 151–167.
29 N. Süleymanoğlu, P. Kubaşık and Ş. Direkel, *J. Chem.*, 2021, **2021**, 1–11.
30 M. J. Frisch, G. W. Trucks, H. B. Schlegel, et al. *Gaussian 16*, Gaussian, Inc., Wallingford CT, 2016.
31 F. Furche, R. Ahlrichs, C. Hättig, W. Klopper, M. Sierka and F. Weigend, *Wiley Interdiscip. Rev. Comput. Mol. Sci.*, 2014, **4**, 91–100.
32 R. Ahlrichs, M. Bär, M. Häser, H. Horn and C. Kölmel, *Chem. Phys. Lett.*, 1989, **162**, 165–169.
33 J. Tao, J. P. Perdew, V. N. Staroverov and G. E. Scuseria, *Phys. Rev. Lett.*, 2003, **91**, 146401.
34 F. Weigend and R. Ahlrichs, *Phys. Chem. Chem. Phys.*, 2005, **7**, 3297.
35 S. Grimme, J. Antony, S. Ehrlich and H. Krieg, *J. Chem. Phys.*, 2010, **132**, 154104.
36 B. Metz, H. Stoll and M. Dolg, *J. Chem. Phys.*, 2000, **113**, 2563–2569.
37 A. V. Marenich, C. J. Cramer and D. G. Truhlar, *J. Phys. Chem. B*, 2009, **113**, 6378–6396.
38 J. Tomasi, B. Mennucci and R. Cammi, *Chem. Rev.*, 2005, **105**, 2999–3094.
39 M. Jansen, *Angew. Chemie*, 1978, **90**, 141–142.
40 B. Shavinsky, L. Levchenko and V. Mitkin, *Chem. Sustain. Dev.*, 2010, **18**, 663–667.
41 C. L. Perrin and J. B. Nielson, *Annu. Rev. Phys. Chem.*, 1997, **48**, 511–544.
42 B. Ndjamen, B.-H. Kang, K. Hatsuzawa and P. E. Kima, *Cell. Microbiol.*, 2010, **12**, 1480–1494.

Graphical abstract